The Role of Canopy Structure in the Spectral Variation of Transmission and Absorption of Solar Radiation in Vegetation Canopies

Oleg Panferov, Yuri Knyazikhin, Ranga B. Myneni, Jörg Szarzynski, Stefan Engwald, Karl G. Schnitzler, and Gode Gravenhorst

***Abstract*—This paper presents empirical and theoretical analyses of spectral hemispherical reflectances and transmittances of individual leaves and the entire canopy sampled at two sites representative of equatorial rainforests and temperate coniferous forests. The empirical analysis indicates that some simple algebraic combinations of leaf and canopy spectral transmittances and reflectances eliminate their dependencies on wavelength through the specification of two canopy-specific wavelength-independent variables. These variables and leaf optical properties govern the energy conservation in vegetation canopies at any given wavelength of the solar spectrum. The presented theoretical development indicates these canopy-specific wavelength-independent variables characterize the capacity of the canopy to intercept and transmit solar radiation under two extreme situations, namely, when individual leaves 1) are completely absorptive and 2) totally reflect and/or transmit the incident radiation. The interactions of photons with the canopy at red and near-infrared (IR) spectral bands approximate these extreme situations well. One can treat the vegetation canopy as a dynamical system and the canopy spectral interception and transmission as dynamical variables. The system has two independent states: canopies with totally absorbing and totally scattering leaves. Intermediate states are a superposition of these pure states. Such an interpretation provides powerful means to accurately specify changes in canopy structure both from ground-based measurements and remotely sensed data. This concept underlies the operational algorithm of global leaf area index (LAI), and the fraction of photosynthetically active radiation absorbed by vegetation developed for the moderate resolution imaging spectroradiometer (MODIS) and multiangle imaging spectroradiometer (MISR) instruments of the Earth Observing System (EOS) Terra mission.**

***Index Terms*—EOS Terra, leaf area index (LAI), multiangle imaging spectroradiometer (MISR), moderate resolution imaging spectroradiometer (MODIS), radiative transfer, vegetation remote sensing.**

Manuscript received August 19, 1999; revised August 1, 2000. This work was supported in part by Bundesministerium für Bildung and Forshung (BMBF), Bonn, Germany, the National Aeronautics and Space Administration (NASA), Washington, DC, Contract NAS5-96061, and the A.F.W Schimper-Foundation, Hohenheim, Germany.

O. Panferov, K. G. Schnitzler, and G. Gravenhorst are with the Institute of Bioclimatology, University Göttingen, D-37077, Göttingen, Germany (e-mail: opanfyo@gwdg.de; schnitzle@gwdg.de; ggraven@gwdg.de).

Y. Knyazikhin and R. B. Myneni are with the Department of Geography, Boston University, Boston, MA 02150 USA (e-mail: jknjazi@crsa.bu.edu; rmyneni@crsa.bu.edu).

J. Szarzynski is with Geographical Institute, Mannheim University, Mannheim, Germany (e-mail: anhuf@rumms.uni-mannheim.de).

S. Engwald is with Botanical Institute, Bonn University, Bonn, Germany (e-mail: s.engwald@gmx.de).

Publisher Item Identifier S 0196-2892(01)01175-5.

I. Introduction

LAND surface processes are important components of the terrestrial climate system. An accurate description of interactions between the surface and the atmosphere requires reliable quantitative information about the fluxes of mass and momentum over terrestrial areas, where they are closely associated with the rates of evapotranspiration and photosynthesis. The vegetation canopy is a special type of surface because of its role in the Earth's energy balance and also, due to its impact on the global carbon cycle. The problem of accurately evaluating the exchange of carbon between the atmosphere and terrestrial vegetation has received scientific [1] and also, political attention [2].

The solar energy that transits through the atmosphere to the vegetation canopy is made available to the atmosphere by reflectance and transformation of radiant energy absorbed by plants and soil into fluxes of sensible and latent heat and thermal radiation through a complicated series of biophysiological, chemical, and physical processes. Therefore, to quantitatively predict the vegetation and atmospheric interactions, it is important to specify those environmental variables that drive the short-wave energy conservation in vegetation canopies. That is, partitioning of the incoming radiation between canopy absorption, transmission, and reflection. Many studies investigated the interaction of solar radiation with vegetation canopies through canopy radiation models (see for example, [3], [4]). Most of them, however, were aimed at examining the scattering behavior of various types of vegetation which is correlated with vegetation-atmosphere processes [5], [6]. In the forests, for example, the interactions of photons with the rough and rather thin surface of tree crowns and also, with the ground exposed through gaps between the crowns, determine the observed variation in the directional reflectance distribution. On the other hand, it is the radiation regime within the canopy that triggers biophysiological, chemical, and physical processes. To a large degree, these influence the exchange of energy, water, and carbon with the atmosphere [6]. Models that account for the scattering properties of vegetation only, although accurate, are not sufficient to describe the radiation regime within vegetation canopies.

The concept of characterizing the state of vegetation canopies via the law of energy conservation arises in the context of remote sensing of vegetation [7], [8]. An algorithm for the estima-

tion of leaf area index (LAI) and fraction of absorbed photosynthetically active radiation (fAPAR) based on the law of energy conservation has been developed and implemented for operational use with moderate resolution imaging spectroradiometer (MODIS) and multiangle imaging spectroradiometer (MISR) data during the Earth Observing System (EOS) Terra mission [9], [10]. A key idea to incorporate the energy conservation law for the retrieval of LAI and fAPAR is the use of eigenvalues of the transport equation to relate optical properties of individual leaves to vegetation canopy transmittance, absorptance, and reflectance. Although this approach was theoretically justified [9], [10] and prototyped with available satellite data [11], [12], no direct evidence of its validity was presented. Our primary objective in this article is to demonstrate the theoretically derived relationships between the eigenvalues of the transport equation; leaf and canopy optical properties are consistent with those derived from measurements. Eigenvalues that drive the short-wave energy conservation in vegetation canopies are measurable parameters. Therefore, our secondary objective is to demonstrate the importance of including systematic measurements of leaf and canopy spectral properties in ground-based observation programs at research stations. This data can be used to accurately specify dynamics of canopy structure changes.

II. Experimental Sites, Instrumentation and Measurements

The hemispherical canopy transmittance (reflectance) for nonisotropic incident radiation is the ratio of the mean downward radiation flux density at the canopy bottom (mean upward radiation flux density at the canopy top) to the downward radiation flux density above the canopy. The hemispherical leaf transmittance (reflectance) is the portion of radiation flux density incident on the leaf surface that the leaf transmits (reflects). The hemispherical leaf albedo is the sum of the hemispherical leaf transmittance and reflectance. All these variables are wavelength dependent. The reflectance and transmittance of an individual leaf depends on the tree species, growth conditions, leaf age, and its location in the canopy space. Described below are the two forest sites with a dark ground chosen to measure leaf and canopy optical properties.

A. Sites and Instruments

1) Forêt des Abeilles Site: This site is an equatorial rainforest at the border of Réserve de La Lopé-Okanda, Gabon (Forêt des Abeilles; 0° 40′ 82″ S and 11° 54′ 65″ E; altitude: 215 m a.s.l.). The measurements were taken during an Operation Canopy La Makande'99 campaign (www.radeau-des-cimes.com). The dominant vegetation type is "Marantaceae-forest" [13], [14], containing typical climbing species of Marantacee (e.g., *Haumania liebrechtsiana*, *Hypselodelphis violaceae* or *Ataenidia conferta*) in the understory. The forest is clearly stratified into three main layers: 1) the understory, up to 10 m high; 2) the lower tree layer (lower canopy), 15 to 20 m, with species such as *Trichoscypha spp*. (Anacardiaceae), *Enantia chlorantha and Polyalthia suaveolens* (both Annonaceae), as well as various Lauraceae (*Ocotea gabonensis*) and Rubiaceae; and 3) the upper tree layer (upper canopy), 30 m and higher (up to 60 m). The mean tree height is about 45 m, and the predominant species is Burseraceae *Aucoumea klaineana* (Okoumé). Other important species are *Dacryoides buettneri* (Burseraceae), *Irvingia gabonensis*, and *I. grandifolia* (Irvingiaceae), various *Dialium* species (Caesalpiniaceae), and other Leguminoses or the giant *Ongokea gore* (Olacaceae).

2) Solling Site: This site is a coniferous (*Picea abies (L.) Karst*) forest in Solling approximately 50 km North–West of Göttingen, Germany ("F1 Fläche;" 51.46° N and 9.35° E, Altitude: 500 m a.s.l.). The forest is nearly 115 years old. The trees average a height of 26 m, with an average crown height of about 11 m. The tree density is 456 trees/ha, and the ground beneath the canopy is a dark soil with litter-fall. A one-year shoot of size 5–7 cm was taken as the basic foliage element ("needle leaf") in this study. This site was selected in 1966 as an experimental region for a "Solling Project" within the EU Program "Experimental Ecology" [15].

3) Instruments: The LI-1800 spectroradiometer with standard cosine receptor was used to measure canopy spectral transmittances and to determine the spectral composition of incoming radiation in the region from 400 nm to 1100 nm, at 1 nm resolution. The instrument was mounted on a tripod with a specially constructed holder to keep the LI-1800 horizontal at about 1 m above the forest floor. The LI-1800-12 external integrating sphere was mounted on LI-1800 to measure the leaf spectral hemispherical transmittances and reflectances. The spectroradiometer was calibrated by means of the LI-1800-02 optical radiation calibrator. In Solling, the canopy spectral hemispherical reflectances were also measured.

B. Field Measurements

All measurements at the Forêt des Abeilles site, Gabon, were performed with one LI-1800 instrument. A rope system was mounted between an *Irvinia grandifolia tree* and a raft [16] that was located on the crown of a *Dialium* sp. First, the instrument was pulled up and the spectral variation of incident radiation flux at the top (nonobscured by tree crowns) was measured. Then it was pulled down and measurements of spectral downward radiation fluxes were taken at six different points located 1 m above the forest floor. The average of these six measurements was taken as the mean downward radiation flux at the canopy bottom. To account for changes in sun position during ground measurements and consequent changes in spectral composition of the incident radiation, a second measurement of the incident spectral flux at the top was taken immediately following the ground measurements. The mean of the two measurements was used to specify the incident spectral flux in the canopy. The mean canopy transmittance was evaluated as the ratio between mean fluxes of transmitted and incident radiation fields. These measurements were carried out on March 3, 1999 between 10:00 and 11:00, and March 4, 1999, between 11:20 and 12:20, under clear sky conditions.

Five leaves from each layer were sampled and their spectral transmittances and reflectances were measured 1 h later under laboratory conditions using the same LI-1800 and the external LI-1800 integrating sphere. For each layer, a pattern of leaf spectral transmittance and reflectance is taken as the average of

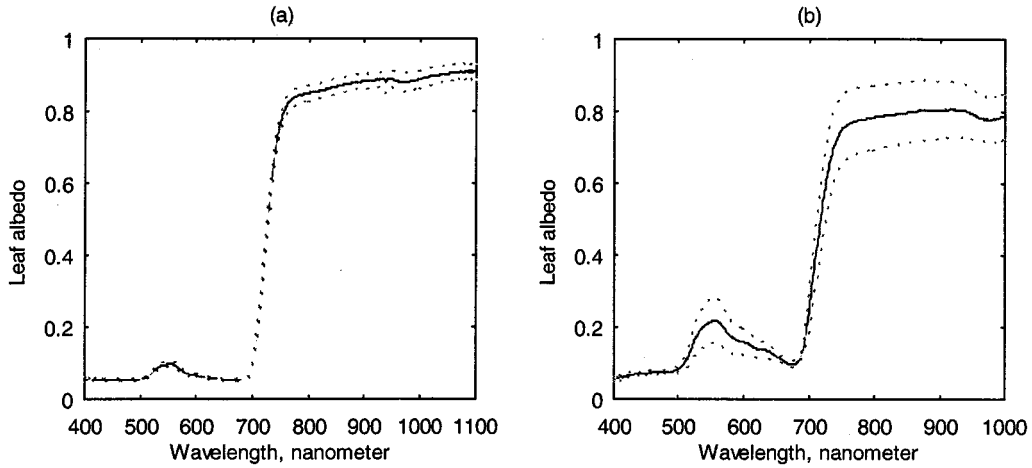

Fig. 1. Mean spectral albedo (solid line) and its standard deviation (dotted line) for leaves in (a) the understory of the Forêt des Abeilles rainforest stand and (b) the entire crown of the Solling coniferous stand. These mean spectral curves were used in all calculations presented in this paper.

the five measurements. Fig. 1(a) shows the leaf spectral albedo (leaf transmittance plus leaf reflectance) and its standard deviation for leaves in the understory of the Forêt des Abeilles rainforest stand.

In Solling, two LI-1800s calibrated to one another were used to measure the canopy spectral transmittances. The first was mounted on top of a 50 m tower [17]. It was programmed to sample the spectral composition of the downward radiation flux every 3 min. The second instrument was used to measure the spectral variation of downward radiation fluxes at six different points, each point 1 m above the forest floor. Six simultaneous measurements of incident and transmitted radiation fluxes were taken on June 4, 1998 between 15:30 and 16:00, and June 6, 1998 between 11:30 and 12:00, under clear sky conditions. For each day, mean spectral downward radiation fluxes at the canopy top and bottom were evaluated using these six simultaneous measurements. The mean canopy transmittance was evaluated as the ratio between mean fluxes of transmitted and incident radiation. On June 4, 1998, the second LI-1800 was mounted on top of the tower to measure upward radiation flux. The spectral variation of upward fluxes was collected between 13:00 and 13:30. The ratio between upward and downward radiation fluxes above the canopy was taken as the canopy reflectance.

One-year shoots of size 5–7 cm with needles of different ages (current year and second year) were sampled from sun and shade parts of crowns. Their spectral transmittances and reflectances were measured one hour later in a laboratory, using the second LI-1800 with the LI-1800-12 external integrating sphere. We followed the standard measurement methodology [18], though no geometrical corrections were made [19]. The spectral curves were separated into four groups with respect to the location of the shoot in the canopy space (sun and shade crown) and needle age (current year and last year). Each group was represented by five spectral curves. From these data, three patterns of mean leaf spectral transmittance and reflectance were derived. They were assumed to represent the optical properties of the leaves in the sun, shade, and the entire crown. Fig. 1(b) demonstrates the mean spectral albedo and its standard deviation of leaves in the whole crown.

III. Canopy Spectral Transmittance and Absorptance: Data Analysis

Let $\mathbf{t}(\lambda)$, $\mathbf{r}(\lambda)$, and $\mathbf{a}(\lambda)$ be the canopy transmittance, reflectance, and absorptance at wavelength λ. These variables are the three basic components of the law of energy conservation. If reflectance of the ground below the vegetation is zero, this law can be expressed as

$$\mathbf{t}(\lambda) + \mathbf{r}(\lambda) + \mathbf{a}(\lambda) = 1 \tag{1}$$

that is, radiation absorbed, transmitted, and reflected by the canopy is equal to radiation incident on the canopy. Let leaf transmittance, reflectance, and albedo at wavelength λ be denoted by $\tau(\lambda)$, $\rho(\lambda)$ and $\omega(\lambda)$, respectively. They are related as

$$\omega(\lambda) = \tau(\lambda) + \rho(\lambda).$$

Let $\mathbf{i}(\lambda)$ be the canopy absorption $\mathbf{a}(\lambda)$ normalized by leaf absorption $1 - \omega(\lambda)$, i.e.,

$$\mathbf{i}(\lambda) = \frac{\mathbf{a}(\lambda)}{1 - \omega(\lambda)} = \frac{1 - \mathbf{t}(\lambda) - \mathbf{r}(\lambda)}{1 - \omega(\lambda)}.$$

For a vegetation canopy bounded at its bottom by a black surface, this variable is the mean number of photon interactions with leaves at wavelength λ before either being absorbed or exiting the canopy. We term this variable canopy interception.

A. Spectral Invariant

We begin the data analysis by examining the variable

$$\xi_\chi(\lambda_0, \lambda_1) = \frac{\chi(\lambda_0) - \chi(\lambda_1)}{\omega(\lambda_0)\chi(\lambda_0) - \omega(\lambda_1)\chi(\lambda_1)} \tag{2}$$

where χ represents either the canopy transmittance, $\mathbf{t}(\lambda)$, canopy interception, $\mathbf{i}(\lambda)$, or canopy reflectance $\mathbf{r}(\lambda)$. Note that $\xi_\chi, \chi = \mathbf{t}, \mathbf{i}$, and $\mathbf{r}$, are symmetrical functions with respect to the spectral variables λ_0 and λ_1. That is, $\xi_\chi(\lambda_0, \lambda_1) = \xi_\chi(\lambda_1, \lambda_0)$. These functions are undefined when $\lambda_0 = \lambda_1$. We consider the case when $\lambda_0 > \lambda_1$. For each day and site, the spaces D_χ,

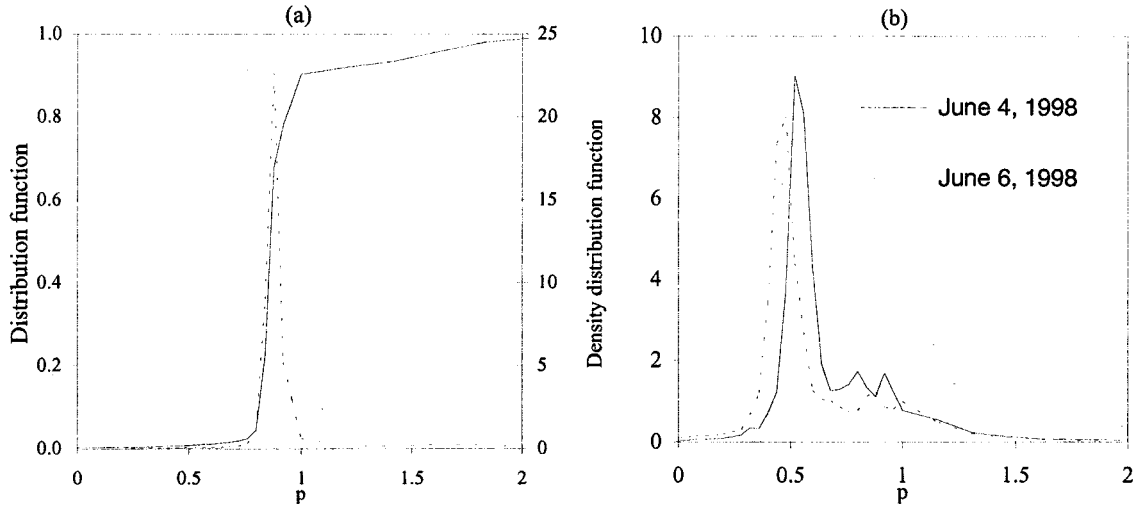

Fig. 2. (a) Cumulative (left axis, solid line) and density distribution functions (right axis, dotted line) of $\xi_{\mathbf{t}}$ [see (2)] derived from data collected at the Forêt des Abeilles site on March 3, 1999. (b) Density distribution functions of $\xi_{\mathbf{t}}$ [see (2)] derived from data collected at the Solling site on June 4, 1998 and June 6, 1998.

$\chi = \mathbf{t}$, $\mathbf{i}$, and $\mathbf{r}$ of realizations of $\xi_\chi(\lambda_0, \lambda_1)$ were created. That is, values of the function $\xi_\chi(\lambda_0, \lambda_1)$ corresponding to all combinations of λ_0 and λ_1, for which $\lambda_0 > \lambda_1$ were calculated. In order to avoid division by zero in (2), values of $\xi_\chi(\lambda_0, \lambda_1)$ corresponding to couples (λ_0, λ_1) for which $|\omega(\lambda_0)\chi(\lambda_0) - \omega(\lambda_1)\chi(\lambda_1)| > 5 \cdot 10^{-4}$ were used. For the Solling site, D_χ included values of $\xi_\chi(\lambda_0, \lambda_1)$ corresponding to the mean spectral albedos of leaves in sun, shade, and the whole crown. For the Forêt des Abeilles site, patterns of mean albedos representing different vertical layers and the entire canopy were used to define D_χ. For each pattern of leaf albedo, histograms of $\xi_\chi(\lambda_0, \lambda_1)$ were derived. Finally, the cumulative distribution functions $F_\chi(p)$ [probability that $\xi_\chi < p$; $0 \leq F_\chi(p) \leq 1$] and density distribution functions $f_\chi(p) = dF_\chi(p)/dp$ were derived from these histograms.

The cumulative and density distribution functions $F_{\mathbf{t}}(p)$ and $f_{\mathbf{t}}(p)$, derived from data collected at the Forêt des Abeilles site on March 3, 1999, are shown in Fig. 2(a). A subset of $D_{\mathbf{t}}$ corresponding to the spectral albedo of leaves in the understory contained 213 341 values of (2). One can see that $F_{\mathbf{t}}(p)$ is very close to the Heaviside function, with a sharp jump from zero to 1 at $p_{\mathbf{t}} \approx 0.88$. The density distribution function $f_{\mathbf{t}}(p)$ behaves as the Dirac delta-function, i.e., $dF_{\mathbf{t}}(p)/dp \approx \delta(p - p_{\mathbf{t}})$. Indeed, 74% of the 213 341 values fell in the interval [0.84, 0.96). 4% and 22% of these values were below 0.84 and above 0.96, respectively. The density distribution function achieved its maximum at $p_{\mathbf{t}} = 0.88$. The distribution functions $F_{\mathbf{t}}(p)$ and $f_{\mathbf{t}}(p)$ corresponding to the same mean albedo and derived from data collected on March 4, 1999, exhibited similar behavior. However, the maximum of $f_{\mathbf{t}}(p)$ was at $p_{\mathbf{t}} = 0.96$. The density distribution functions $f_{\mathbf{t}}(p)$ derived from data collected at the Solling site on June 4, 1998, between 15:30 and 16:00 and June 6, 1998, between 11:30 and 12:00, are shown in Fig. 2(b). The space $D_{\mathbf{t}}$ was formed from values of $\xi_{\mathbf{t}}(\lambda_0, \lambda_1)$ corresponding to spectral variables from the interval [550 nm, 1000 nm]. Values of $p_{\mathbf{t}}$, at which the density distribution functions reached their maximum were 0.52 (June 4, 1998) and 0.48 (June 6, 1998). Thus, the most probable value of $\xi_{\mathbf{t}}$ is strongly sensitive to the canopy structure and slightly to sun position. Fig. 3 (dotted line) demonstrates the density distribution function $f_{\mathbf{r}}(p)$ for the canopy reflectance derived from Solling data. Combinations of (λ_0, λ_1) were formed from the interval [550 nm, 1000 nm], and the mean spectral albedo of leaves in the entire crown was used. The maximum of $f_{\mathbf{r}}(p)$ was at $p_{\mathbf{r}} = 0.92$. Solid line in Fig. 3 illustrates the density distribution function $f_{\mathbf{i}}(p)$ the for canopy interception derived from Solling data (June 4, 1998) using the same pattern of leaf spectral albedo and the spectral interval [400 nm, 1000 nm]. The interval [0.92, 1] contained 79% of 170 405 values in the space $D_{\mathbf{i}}$, maximum of $f_{\mathbf{i}}(p)$ was at $p_{\mathbf{i}} = 0.94$. Thus, with a high probability, the variables (2) are wavelength independent, i.e., ξ_χ is invariant with respect to the wavelength.

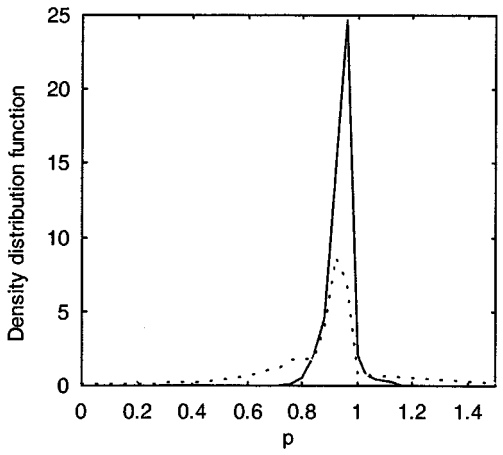

Fig. 3. Density distribution functions of $\xi_{\mathbf{i}}$ (solid line) and $\xi_{\mathbf{r}}$ (dotted line) derived from data collected at the Solling site on June 4, 1998.

B. Spectral Variation of Canopy Transmittance and Absorptance

Results presented in Section III-A indicate that simple algebraic combinations of leaf and canopy spectral transmittances and reflectances are only slightly sensitive to the wavelength.

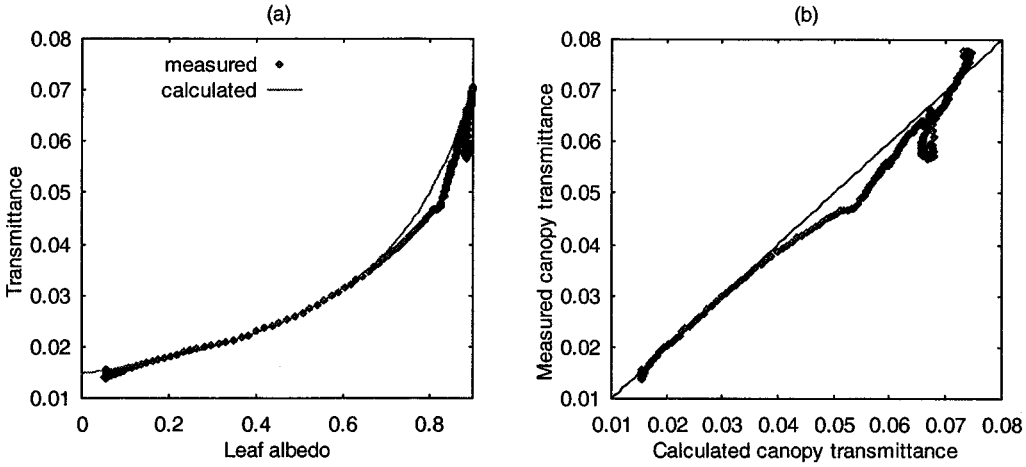

Fig. 4. (a) Measured and calculated canopy spectral transmittances and (b) their correlation for the Forêt des Abeilles site on March 3, 1999.

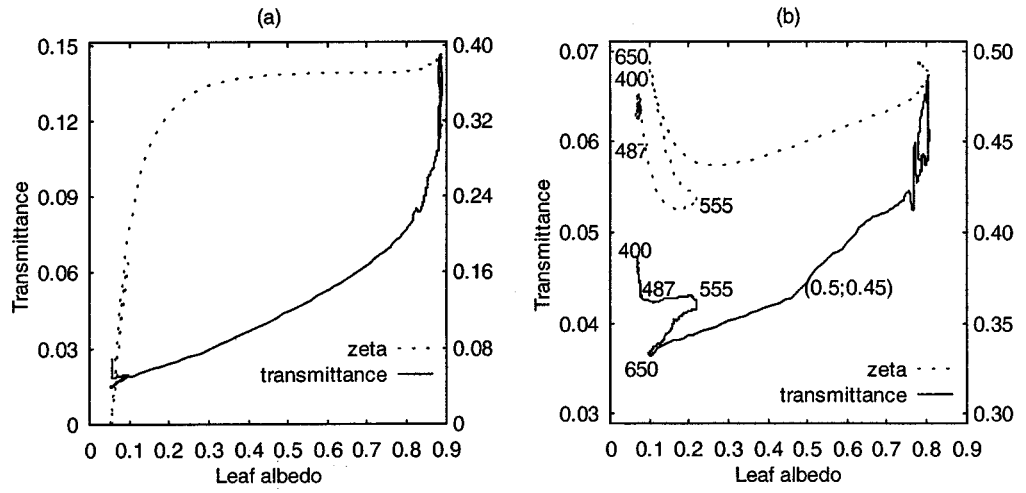

Fig. 5. Canopy transmittance $\mathbf{t}$ (left axis) and the ratio ζ of the leaf transmittance to the leaf albedo (right axis, legend "zeta") as functions of leaf albedo ω derived from (a) the Forêt des Abeilles (March 4, 1999) and (b) Solling (June 6, 1998) data. The labels "400," "487," "555," and "650" depict couples $[\omega(\lambda), \mathbf{t}(\lambda)]$ and $[\omega(\lambda), \zeta(\lambda)]$ of measured leaf albedo $\omega(\lambda)$, canopy transmittance $\mathbf{t}(\lambda)$, and the ratio $\zeta(\lambda)$ at 400 nm, 487 nm, 555 nm, and 650 nm, respectively. The label "(0.5; 0.45)" separates a value of the canopy transmittance corresponding to $\omega = 0.5$ and $\zeta = 0.45$. One can see that $\mathbf{t}$ and ζ take on multiple values simultaneously.

TABLE I
COEFFICIENT p_t AS A FUNCTION OF EXPERIMENTAL SITE AND PATTERN OF MEAN LEAF SPECTRAL ALBEDO

Pattern of mean leaf spectral albedo	p_t	RMSE	p_t	RMSE
Solling site (Germany)	June 04, 1998		June 06, 1998	
Sun crown	0.51	0.0049	0.41	0.0073
Shade crown	0.61	0.0044	0.47	0.0071
Whole crown	0.54	0.0041	0.48	0.0067
Forêt des Abeilles site (Gabon)	March 03, 1999		March 04, 1999	
Upper tree layer	0.86	0.0104	0.895	0.057
Lower tree layer	0.84	0.0087	0.926	0.043
Understory	0.88	0.0038	0.957	0.017
Whole canopy	0.854	0.0071	0.931	0.033

Let p_χ, $\chi = \mathbf{t}, \mathbf{i}$, and $\mathbf{r}$ be mathematical expectations of ξ_χ. Resolving (2) with respect to $\chi(\lambda)$, one obtains the most probable canopy spectral transmittance ($\chi = \mathbf{t}$), interception ($\chi = \mathbf{i}$), and reflectance ($\chi = \mathbf{r}$) as

$$\chi(\lambda) = \frac{1 - p_\chi \omega(\lambda_0)}{1 - p_\chi \omega(\lambda)} \chi(\lambda_0). \tag{3}$$

If our hypothesis about the invariance of (2) is correct, one can evaluate canopy transmittance, reflectance, and absorptance $\mathbf{a}(\lambda) = [1 - \omega(\lambda)]\mathbf{i}(\lambda)$ at any wavelength once these variables are known at a reference wavelength λ_0. It will be shown in this section that (3) can be used to evaluate canopy transmittance and interception (and, consequently, canopy absorptance) but not canopy reflectance. For each experimental site, we solved the following problem: given the pattern of mean leaf spectral albedo (defined in Section II-B), find p_χ such that the disagreement between measured values of $\chi(\lambda)$ and those evaluated with (3) is minimized. Table I presents coefficient $p_\mathbf{t}$ as a function of the site and pattern of mean leaf spectral albedo. For the Solling site, the best values of $p_\mathbf{t}$ were 0.54 (June 4, 1998) and 0.48 (June 6, 1998). Both of these correspond to the needle mean spectral albedo averaged over the entire tree crown. Mean spectral albedo of understory leaves provided the best agreement between measured and evaluated canopy spectral transmittances in the case of the Forêt des Abeilles site. Values of $p_\mathbf{t}$ were 0.88 (March 3, 1999) and 0.957 (March 4, 1999). Fig. 4 demonstrates measured and calculated canopy spectral transmittances and their correlation for the Forêt des Abeilles site on March

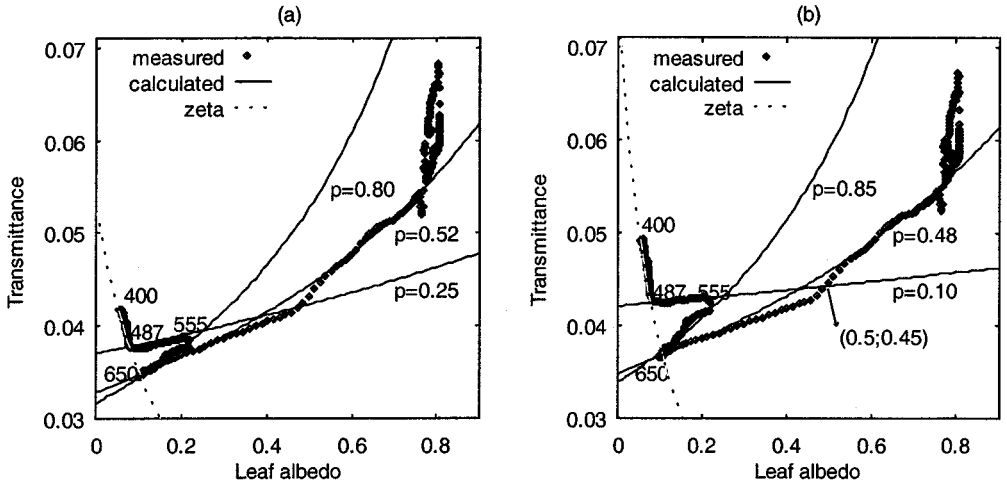

Fig. 6. Measured (legend "measured") and calculated (legend "calculated") canopy transmittances versus leaf albedo for the Solling site on (a) June 4, 1998 and (b) June 6, 1998. The meaning of the labels "400," "487," "555," "650," and "(0.5; 0.45)" is the same as in Fig. 5(b). The curve "zeta" connects measured couples $[\omega(\lambda),\ \mathbf{t}(\lambda)]$ corresponding to 400 nm $\leq \lambda \leq$ 487 nm and $\lambda = 650$ nm. At these wavelengths, the coefficient $\zeta(\lambda)$ varies considerably with $\omega(\lambda)$ almost unchanged [Fig. 5(b)]. Different parts of the canopy transmittance can be approximated by (3) with different values of the parameter $p_{\mathbf{t}}$. Each approximation starts from the curve "zeta," i.e., given canopy transmittances at a reference leaf albedo $\omega_0 = \omega(\lambda_0)$ for different values of $\zeta = \tau(\lambda_0)/\omega_0$, one can find canopy transmittance for any other leaf albedo. Measured leaf albedos and canopy transmittances $[\omega(\lambda),\ \mathbf{t}(\lambda)]$ lying on the curves "$p = 0.80$" (panel a) and "$p = 0.85$" (panel b) cause a local maximum of the distribution functions $f_{\mathbf{t}}(p)$ at $p = 0.80$ [Fig. 2(b), solid line] and $p = 0.85$ [Fig. 2(b), dotted line].

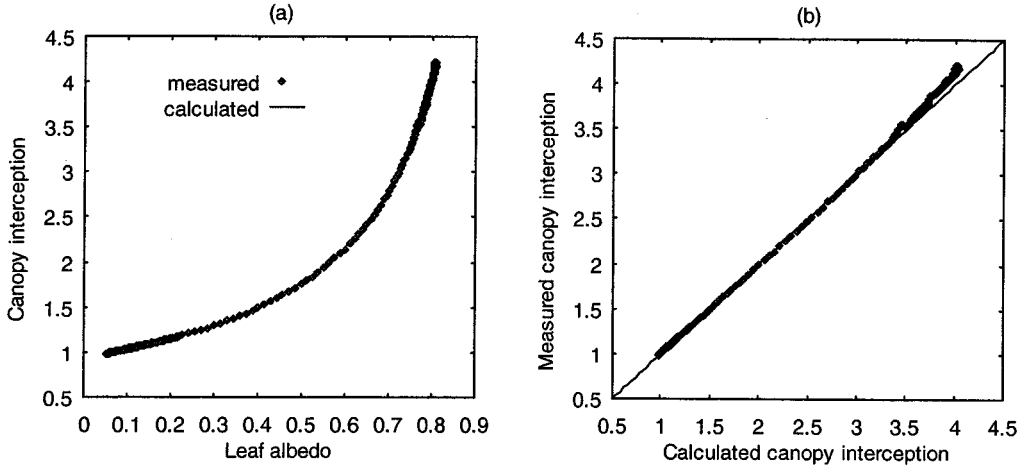

Fig. 7. (a) Measured and calculated canopy spectral interceptions and (b) their correlation for the Solling site on June 4, 1998; $p_{\mathbf{i}} = 0.94$.

3, 1999. A one-to-one correspondence between leaf albedo and canopy transmittance can be observed for almost all values of leaf albedo. Each plot in Fig. 5 contains two curves. The first, with the left vertical axis shows the transmittance as a function of leaf albedo, and the second, with the right vertical axis, illustrates the ratio ζ of leaf transmittance τ to leaf albedo, i.e., $\zeta = \tau/\omega$, as a function of leaf albedo. One can see the functions $\mathbf{t}$ and ζ take on multiple values simultaneously. However, if canopy transmittances at a reference leaf albedo $\omega_0 = \omega(\lambda_0)$ for different values of $\zeta = \tau(\lambda_0)/\omega_0$ are known one can easily find canopy transmittance at any other leaf albedo (Fig. 6). For example, a value of the canopy transmittance at $\omega = 0.5$ and $\zeta = 0.45$ [the point labeled "(0.5; 0.45)" in Fig. 6(b)] can be evaluated with (3) using canopy transmittance at $\omega = 0.1$ and $\zeta = 0.45$ [the point labeled as "487" in Fig. 6(b)] and the parameter $p_t = 0.10$ [the curve "$p = 0.10$" in Fig. 6(b)].

Fig. 7 demonstrates measured and calculated canopy spectral interceptions and their correlation for the Solling site on June 4, 1998. One can see that (3) approximates the canopy spectral interception accurately. Given canopy interception, canopy spectral absorptance can be evaluated as $\mathbf{a}(\lambda) = [1-\omega(\lambda)]\mathbf{i}(\lambda)$. Substituting this expression into (3), one obtains the following formula for canopy spectral absorptance [9]

$$\mathbf{a}(\lambda) = \frac{1 - p_i\omega(\lambda_0)}{1 - p_i\omega(\lambda)} \frac{1 - \omega(\lambda)}{1 - \omega(\lambda_0)} \mathbf{a}(\lambda_0). \tag{4}$$

Fig. 8(a) shows measured and calculated canopy spectral absorptances for the Solling site.

Calculations presented in Section III-A indicate the density distribution function $f_{\mathbf{r}}(p)$ for canopy reflectance localizes some values of $\xi_{\mathbf{r}}$ (Fig. 3). Although the measured and calculated reflectances are sufficiently close to each other [Fig. 8(b)], (3) cannot be used to approximate canopy spectral reflectance. Indeed, let us assume that this describes the physics of the radiative transfer process correctly. It follows from this

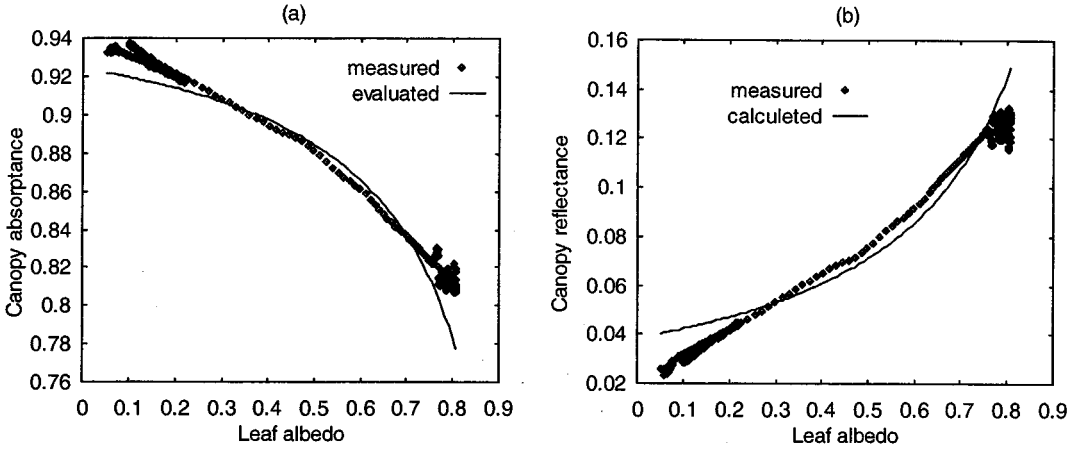

Fig. 8. Measured and calculated canopy (a) absorptances and (b) reflectances as a function of leaf albedo for the Solling site on June 4, 1998; $p_{\mathbf{i}} = 0.94$, $p_{\mathbf{r}} = 0.96$.

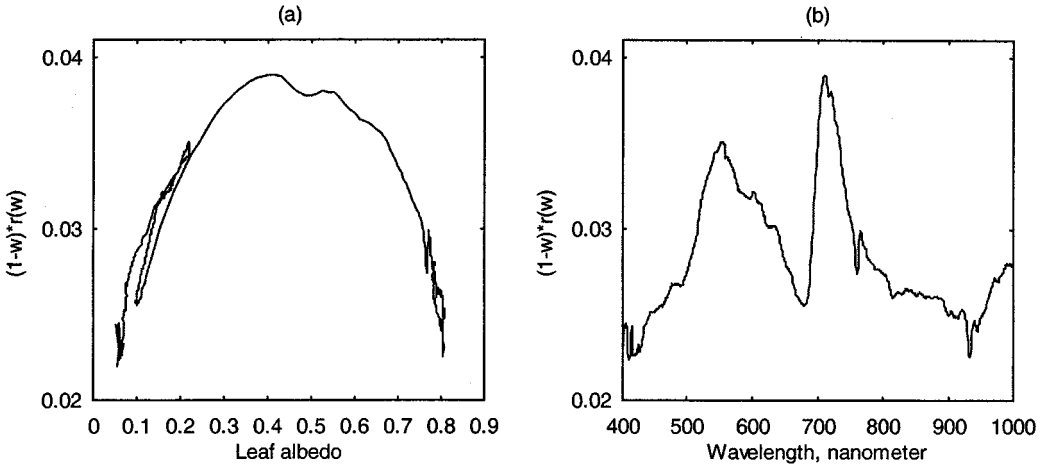

Fig. 9. Weighted canopy transmittance $[1-\omega]\mathbf{r}(\omega)$ as a function of (a) leaf albedo and (b) wavelength derived from Solling data (June 4, 1998).

assumption that $(1-\omega)\mathbf{r}(\omega)$ is either a decreasing (if $p_{\mathbf{r}} < 1$) or increasing (if $p_{\mathbf{r}} > 1$) function with respect to ω. Fig. 9(a) shows the function $(1-\omega)\mathbf{r}(\omega)$ derived from Solling data. One can see that our assumption contradicts the measurements. Thus, the use of (3) to simulate spectral variation of canopy reflectance can lead to a wrong interpretation of the radiative transfer process in vegetation canopies.

Why does the density distribution function $f_{\mathbf{r}}(p)$ localize some values of $\xi_{\mathbf{r}}$? One can see from Fig. 9(a) that $(1-\omega)\mathbf{r}(\omega)$ is a nearly symmetrical function relative to $\omega \approx 0.4$. That is, it takes approximately the same values at $\omega(\lambda_0) = 0.4 + \omega$ and $\omega(\lambda_1) = 0.4 - \omega$. The variable $\xi_{\mathbf{r}}$ takes a value of about 1 in this case. About half of couples $[\omega(\lambda_1), \omega(\lambda_2)]$ corresponding to different (λ_0, λ_1) satisfy the condition $0.4 - \omega(\lambda_0) \approx 0.4 + \omega(\lambda_1)$ [Figs. 1(b) and 9(b)]. As a result, about 52% of $\xi_{\mathbf{r}}$ values fall in the interval [0.92, 1). Thus, in this particular case, the symmetry of $(1-\omega)\mathbf{r}(\omega)$ results in a localization of $\xi_{\mathbf{r}}$ values. This example demonstrates that a good fit between measured and modeled canopy reflectances is not a sufficient argument to relate such a model to the physical process; that is, such a model can still violate the law of energy conservation. The canopy spectral interception, transmittance and absorptance data are consistent with the behavior of $(1-\omega)\chi(\omega)$, $\chi = \mathbf{t}, \mathbf{i}$, indicated by (3) [Figs. 8(a), 10(a) and (b)].

Recall, the upward flux of canopy leaving radiation was measured at one spatial point above the forest stand (Section II-B), resulting in a rather high uncertainty in the measured canopy spectral reflectance [17]. The effect of this uncertainty on the canopy spectral absorptance is not quit discernible [Fig. 10(b)]. However, values of $(1-\omega)\mathbf{r}(\omega)$ derived from a particular measurement of canopy spectral reflectance can greatly differ from those obtained by resolving the energy conservation law (1) with respect to $\mathbf{r}$ and using (3) to evaluate canopy spectral transmittance and absorptance. Fig. 13(c) shows the weighted canopy reflectances $(1-\omega)\mathbf{r}(\omega)$ versus the mean albedo of a leaf in coniferous tree crowns for three patterns of the weight $(1-\omega)$ derived from the Solling data. Essential variations in the shape of $(1-\omega)\mathbf{r}(\omega)$ can be seen and consequently, the points at which $(1-\omega)\mathbf{r}(\omega)$ reaches its maximum can clearly be seen. Although not enough data were collected to evaluate the mean canopy reflectance accurately, the canopy reflectance calculated with (1) and (3) reflects the correct tendency in the behavior of data. That is, $(1-\omega)\mathbf{r}(\omega)$ is not a monotonic function with respect to the leaf albedo ω [Fig. 10(c)]. This finding suggests that focusing on the development of canopy radiation models without accounting

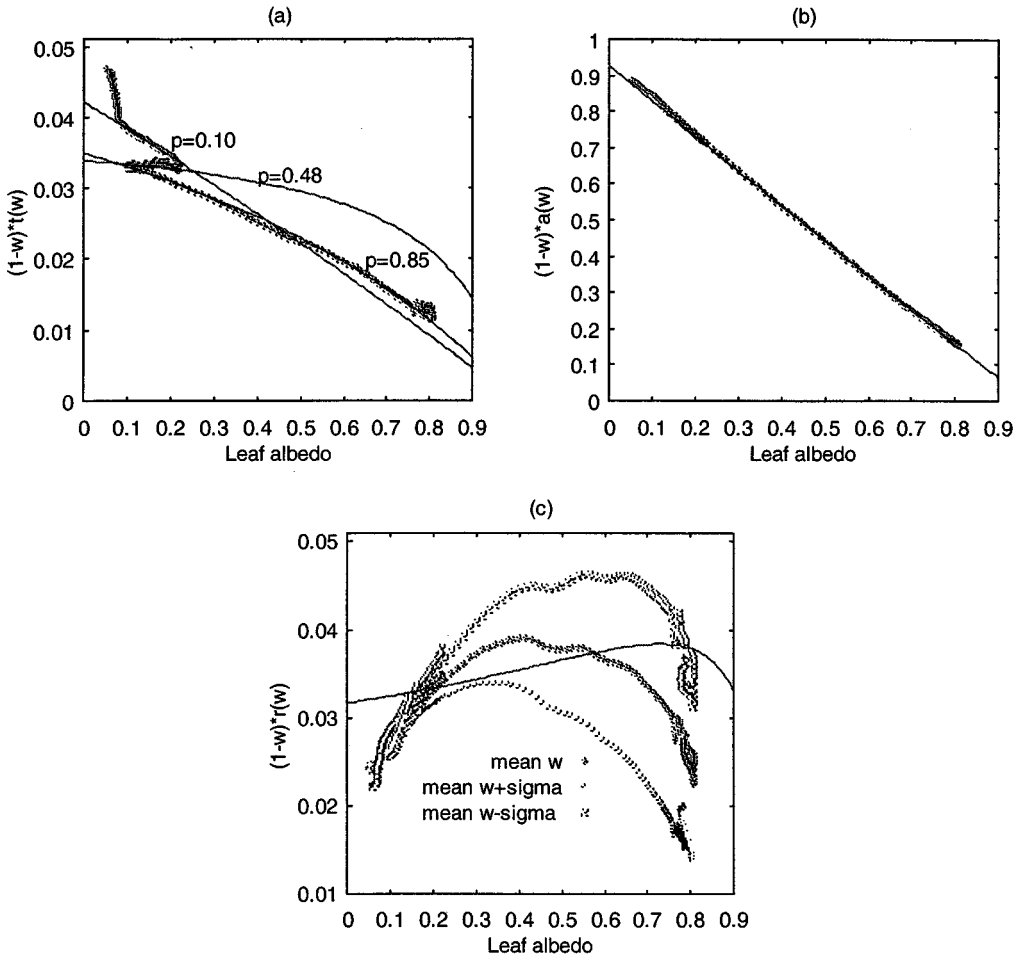

Fig. 10. Weighted canopy (a) transmittance $(1-\omega)\mathbf{t}(\omega)$, (b) absorptance $(1-\omega)\mathbf{a}(\omega)$, and (c) reflectance $(1-\omega)\mathbf{r}(\omega)$ derived from Solling data on June 4, 1998 (points) and calculated (lines) with (3). Patterns of spectral leaf albedo shown in Fig. 1(b) were used to plot measured values of $(1-\omega)\mathbf{r}$ versus the mean albedo of a leaf in coniferous tree crowns, namely, the mean albedo ω of a leaf in coniferous tree crowns (legend "mean w"), and $\omega \pm \sigma$ (legends "mean w + sigma" and "mean w − sigma," respectively). Here, σ is the dispersion of ω. The meaning of the labels "$p = 0.10$," "$p = 0.48$," and "$p = 0.85$" is the same as in Fig. 6.

for canopy transmittance and absorptance (which are sensitive to the within-canopy radiation regime) can lead to an incorrect interpretation of measured data.

Thus, the energy conservation in vegetation canopies at a given band of the solar spectrum is driven by optical properties of individual leaves at this spectral band and two wavelength independent structural parameters. Simple algebraic combinations of leaf and canopy spectral transmittances and reflectances which eliminate their dependencies on wavelength determine the structural variables. Given canopy optical properties of an individual leaf, two structural variables and canopy transmittance and absorptance at a reference wavelength, the correct proportion of canopy absorptance, transmittance and reflectance can be found at any wavelength of the solar spectrum. The following section presents a theoretical justification of this statement.

IV. Canopy Spectral Transmittance and Absorptance: Theory

Analysis presented in Section III indicates that the cumulative distribution functions of random variables ξ_χ, $\chi = \mathbf{t}$, and $\mathbf{i}$, can be described by the Heaviside function. This means expression (2) does not depend upon wavelength. That is, they are invariant with respect to the spectral variable. In this section, we develop theoretical arguments to interpret the physical meaning of the points at which the cumulative distribution functions of ξ_χ, $\chi = \mathbf{t}$, and $\mathbf{i}$ jump from zero to 1. The analysis is based on the following physical concept: the measurement of a dynamical variable must result in an eigenvalue of a linear operator representing that dynamical variable. The state in which the dynamical variable has that value is represented by the corresponding eigenvector [20]. In the case of canopy transmittance, an operator that assigns downward radiances at the canopy bottom to incoming radiation can be taken as the linear operator representing the transmittance process. An operator that sets in correspondence to the incoming radiation, a three-dimensional (3-D) radiation field within the canopy can be taken to represent the interception process. The equation of radiative transfer in the vegetation canopy [21] is used to specify these operators.

A. Radiative Transfer Problem for Vegetation Media

Consider a vegetation canopy in the layer $0 < z < H$. The top $z = 0$ and bottom $z = H$ surfaces form its upper and lower boundaries. The position vector r denotes the Cartesian triplet

(x, y, z) with its origin at the canopy top. Assume that photons interact with phytoelements only. That is, photon interactions with the optically active elements of the atmosphere inside the layer are ignored. The radiation field in the vegetation canopy can be described by the 3-D transport [22]–[24], namely

$$\Omega \bullet \nabla I_\lambda(r, \Omega) + u_L(r) G(r, \Omega) I_\lambda(r, \Omega) = u_L(r) \int_{4\pi} \frac{1}{\pi} \Gamma_\lambda(r, \Omega' \to \Omega) I_\lambda(r, \Omega')\, d\Omega'. \quad (5)$$

Here I_λ is the monochromatic radiance which depends on wavelength λ, location r and direction Ω. The unit vector Ω is expressed in spherical coordinates with respect to $(-Z)$ axis and $\cos^{-1}\ \mu$ and ϕ are its polar angle and azimuth. u_L is the leaf area density distribution function, G is the projection of leaf normals at r onto a plane perpendicular to the direction Ω, and Γ_λ is the area scattering phase function [22]. A precise description of these variables can be found in [22], [23]. Below, the formulation of [23] is adopted.

Equation (5) is a statement of the energy conservation law in the phase space (r, Ω). The first term characterizes the change in radiance along Ω at r, the other terms show whether the changes take place at the expense of absorption and scattering in the vegetation canopy (second term) at the expense of the scattering from other direction into Ω (third term). The wavelength independent function $\sigma(r, \Omega) = u_L(r) G(r, \Omega)$ is the total interaction cross-section (attenuation coefficient). This cross-section is the sum of wavelength dependent scattering $\sigma_{s,\lambda}(r, \Omega)$ and absorption $\sigma_{a,\lambda}(r, \Omega)$ coefficients, i.e.,

$$\sigma(r, \Omega) = \sigma_{s,\lambda}(r, \Omega) + \sigma_{a,\lambda}(r, \Omega). \quad (6)$$

The scattering coefficient is defined as [21]

$$\sigma_{s,\lambda}(r, \Omega) = u_L(r) \int_{4\pi} \frac{1}{\pi} \Gamma_\lambda(r, \Omega \to \Omega')\, d\Omega'.$$

Here the integration is performed over the whole sphere 4π. The absorption coefficient then can be specified from (6). The magnitude of scattering by the elements of the vegetation canopy is described using the hemispherical leaf albedo

$$\omega_\lambda(r, \Omega) = \frac{\sigma_{s,\lambda}(r, \Omega)}{\sigma_{s,\lambda}(r, \Omega) + \sigma_{a,\lambda}(r, \Omega)} = \frac{1}{\pi} \frac{\int_{4\pi} \Gamma_\lambda(r, \Omega \to \Omega')\, d\Omega'}{G(r, \Omega)}. \quad (7)$$

An individual leaf is assumed to reflect and transmit the intercepted energy in a cosine distribution about the leaf normal. In this case, the hemispherical leaf albedo ω_λ is not dependent upon the angular variable Ω. The area scattering phase function Γ_λ is a symmetrical function with respect to angular variables [25] and the reciprocity property $\Gamma_\lambda(r, \Omega' \to \Omega) = \Gamma_\lambda(r, -\Omega' \to -\Omega)$ is locally valid.

Let a parallel beam and diffuse radiation be incident on the upper boundary. Reflectance of the ground underneath the vegetation canopy is assumed to be zero. This case is given by the following boundary conditions:

$$I_\lambda(r_0, \Omega) = j_\lambda(\Omega) \text{ (for downward directions)} \quad (8)$$

$$I_\lambda(r_H, \Omega) = 0 \text{ (for upward directions).} \quad (9)$$

Here r_0 and r_H denote points on the upper and lower boundaries, respectively, and j_λ is the intensity of incident (direct and diffuse) radiation. The solution of the boundary value problem expressed by (5), (8), and (9) describes the radiation field in 3-D forests [24], [26].

Field measurements described in Section II provided the spatial distribution of the following variables: 1) spectral variation of downward ($F^{\downarrow}_{0,\lambda}$) and upward ($F^{\uparrow}_{0,\lambda}$) radiation fluxes above the forest

$$F^{\downarrow}_{0,\lambda} = \int_{\mu<0} j_\lambda(\Omega)|\mu|\, d\Omega$$

$$F^{\uparrow}_{0,\lambda} = \int_{\mu>0} I_\lambda(r_0, \Omega)|\mu|\, d\Omega$$

where $I_\lambda(r, \Omega)$ is the solution of the boundary value problem (5), (8)–(9), 2) spectral variation of downward radiation flux $F^{\downarrow}_{H,\lambda}$ at the canopy bottom, that is

$$F^{\downarrow}_{H,\lambda}(r_H) = \int_{\mu<0} I_\lambda(r_H, \Omega)|\mu|\, d\Omega \quad (10)$$

and 3) hemispherical spectral leaf albedo $\omega_\lambda(r)$. In terms of these notations, canopy transmittance $\mathbf{t}$, reflectance $\mathbf{r}$, and interception $\mathbf{i}$ can be expressed as

$$\mathbf{t}(\lambda) = \frac{\langle F^{\downarrow}_{H,\lambda}(r_H)\rangle_H}{F^{\downarrow}_{0,\lambda}}, \quad \mathbf{r}(\lambda) = \frac{\langle F^{\uparrow}_{0,\lambda}\rangle_0}{F^{\downarrow}_{0,\lambda}}$$

$$\mathbf{i}(\lambda) = \frac{\int_V \int_{4\pi} \sigma(r, \Omega) I_\lambda(r, \Omega)\, d\Omega\, dr}{S F^{\downarrow}_{0,\lambda}}.$$

Here $\langle\rangle_H$ and $\langle\rangle_0$ denote the mean over the bottom and top canopy boundary, V is a domain in which the vegetation canopy is located, and S is the area of the top canopy boundary. All the measured variables are related via the energy conservation law [i.e., the transport (5) and boundary conditions (8) and (9)]. Our goal is to explain the empirical relations derived in Section III using this basic physical principle.

B. Scattering Process in Vegetation Media

Assumptions formulated in the previous subsection are sufficient to precisely derive spectral variation of canopy interception from the 3-D transport equations. That is, (2) for $\chi = \mathbf{i}$ does not depend on spectral variables [9]. A similar statement was formulated earlier for canopy transmittance [9], but no theoretical justification of its validity was presented. The aim of this subsection is to formulate certain additional assumptions that allow the derivation of the spectral variation of canopy transmittance. For simplicity, specular reflection by leaves is ignored, which is not critical to the following analysis.

The area scattering phase function can be expressed as [21]

$$\begin{aligned}\Gamma_\lambda(r, \Omega' \to \Omega) = \frac{1}{2\pi} &\int_{(\Omega\bullet\Omega_L)(\Omega'\bullet\Omega_L)>0} \\ &\cdot t_{L,\lambda}(r, \Omega', \Omega) g_L(r, \Omega_L) \\ &\cdot (\Omega\bullet\Omega_L)(\Omega'\bullet\Omega_L)\, d\Omega_L \\ &+ \frac{1}{2\pi} \int_{(\Omega\bullet\Omega_L)(\Omega'\bullet\Omega_L)<0} \\ &\cdot r_{L,\lambda}(r, \Omega', \Omega) g_L(r, \Omega_L) \\ &\cdot |(\Omega\bullet\Omega_L)(\Omega'\bullet\Omega_L)|\, d\Omega_L.\end{aligned}$$

Here, Ω_L is the outward normal to the leaf surface, g_L is the probability density of the leaf's normal distribution over the upper hemisphere, $r_{L,\lambda}$ and $t_{L,\lambda}$ are the bidirectional reflectance and transmittance factors of an individual leaf, which are assumed Lambertian, i.e., $r_{L,\lambda}(r, \Omega', \Omega) = \rho(\lambda, r)$ and $t_{L,\lambda}(r, \Omega', \Omega) = \tau(\lambda, r)$, where ρ and τ are the leaf hemispherical reflectance and transmittance, respectively. The variables ρ and τ were measured at both the sites described in Section II. Under these assumptions, the area scattering phase function can be expressed as

$$\begin{aligned}&\Gamma_\lambda(r, \Omega' \to \Omega) \\ &\quad = \tau(\lambda, r)\Gamma^+(r, \Omega' \to \Omega) + \rho(\lambda, r)\Gamma^-(r, \Omega' \to \Omega) \quad (11)\end{aligned}$$

where Γ^+ and Γ^- are wavelength independent functions defined as

$$\begin{aligned}\Gamma^\pm(r, \Omega' \to \Omega) = \frac{1}{2\pi} &\int_{\pm(\Omega\bullet\Omega_L)(\Omega'\bullet\Omega_L)>0} \\ &\cdot g_L(r, \Omega_L)|(\Omega\bullet\Omega_L)(\Omega'\bullet\Omega_L)|\, d\Omega_L.\end{aligned}$$

It follows from (7) and (11) that the hemispherical leaf albedo can be expressed as [21]

$$\omega_\lambda(r) = \rho(\lambda, r) + \tau(\lambda, r).$$

The spectral leaf reflectance and transmittance are assumed independent of the spatial variable r.

Differentiating (5) and boundary conditions (8)–(9) with respect to ρ and τ and accounting for (11), one can obtain that the function

$$v(r, \Omega; \rho, \tau) = \rho\frac{\partial I_\lambda(r, \Omega)}{\partial\rho} + \tau\frac{\partial I_\lambda(r, \Omega)}{\partial\tau}$$

satisfies the equation

$$\begin{aligned}&\Omega\bullet\nabla v + u_L(r)G(r, \Omega)v \\ &\quad = \left[\rho\frac{\partial}{\partial\rho} + \tau\frac{\partial}{\partial\tau}\right] u_L(r) \\ &\qquad \cdot \int_{4\pi} \frac{1}{\pi}\Gamma_\lambda(r, \Omega' \to \Omega) I_\lambda(r, \Omega')\, d\Omega' \qquad (12)\end{aligned}$$

and the boundary conditions $v(r_0, \Omega; \rho, \tau) = 0$ for downward directions, and $v(r_H, \Omega; \rho, \tau) = 0$ for upward directions.

C. Eigenvalues and Eigenvectors of the Transport Equation

An eigenvalue of the transport is a number θ such that there exists a function φ that satisfies

$$\begin{aligned}&\theta[\Omega\bullet\nabla\varphi(r, \Omega) + \sigma(r, \Omega)\varphi(r, \Omega)] \\ &\quad = \int_{4\pi} q(r, \Omega' \to \Omega)\varphi(r, \Omega')\, d\Omega' \qquad (13)\end{aligned}$$

with vacuum boundary conditions. Here, q denotes $\pi^{-1}u_L\Gamma_\lambda$. Under some general conditions [27], the set of eigenvalues θ_k, $k = 0, 1, 2, \cdots$ and eigenvectors $\varphi_k(r, \Omega)$, $k = 0, 1, 2, \cdots$ is a discrete set. The eigenvectors satisfy the condition of orthogonality. The transport equation has a unique positive eigenvalue that corresponds to a unique positive eigenvector. This eigenvalue is greater than the absolute magnitudes of the remaining eigenvalues. This means that only one eigenvector, i.e., φ_0, takes on positive values for any r and Ω.

We expand the solution of the transport equation in eigenvectors, namely

$$\begin{aligned}I_\lambda(r, \Omega)/F^\downarrow_{0,\lambda} &= a_0(\rho, \tau)\varphi_0(\rho, \tau; r, \Omega) \\ &\quad + \sum_{k=1}^{\infty} a_k(\rho, \tau)\varphi_k(\rho, \tau; r, \Omega) \qquad (14)\end{aligned}$$

where the coefficients a_k do not depend on spatial or angular variables. Here we separate the positive eigenvector φ_0 into the first summand. Substituting (14) into (12) and accounting for (13) results in

$$\begin{aligned}&[\Omega\bullet\nabla + \sigma(r, \Omega)] \\ &\quad = \sum_{k=0}^{\infty}\left\{\rho\frac{\partial(1-\theta_k)a_k\varphi_k}{\partial\rho} + \tau\frac{\partial(1-\theta_k)a_k\varphi_k}{\partial\tau}\right\} = 0.\end{aligned}$$

Here $\theta_k(\rho, \tau)$ is the eigenvalue corresponding to the eigenvector φ_k. It follows from this equation that

$$\begin{aligned}&\rho\frac{\partial(1-\theta_k)a_k\varphi_k}{\partial\rho} + \tau\frac{\partial(1-\theta_k)a_k\varphi_k}{\partial\tau} = 0 \\ &\quad k = 0, 1, 2, \cdots. \qquad (15)\end{aligned}$$

The general solution of the first order partial (15) with respect to the function $(1-\theta_k)a_k\varphi_k$ can be expressed as [28]

$$[1-\theta_k(\rho, \tau)]a_k(\rho, \tau)\varphi_k(r, \Omega; \rho, \tau) = f_k(\rho/\tau) \qquad (16)$$

where $\rho/\tau = const$ is the characteristic curve of (15), and f_k is an arbitrary function of one variable. Letting $x = \rho/\tau$ and $\omega_0 = \rho + \tau$, one can specify this function as

$$\begin{aligned}f_k(x) = &\left[1 - \theta_k\left(\omega_0\frac{1}{x+1}, \omega_0\frac{x}{x+1}\right)\right] \\ &\cdot a_k\left(\omega_0\frac{1}{x+1}, \omega_0\frac{x}{x+1}\right) \\ &\cdot \varphi_k\left(\omega_0\frac{1}{x+1}, \omega_0\frac{x}{x+1}\right).\end{aligned}$$

Substituting this function into (15), one obtains

$$\begin{aligned}a_k(\rho, \tau)\varphi_k(\rho, \tau) &= \frac{f_k(\rho/\tau)}{1-\theta_k(\rho, \tau)} \\ &= \frac{1-\theta_k(\varsigma\omega_0, (1-\varsigma)\omega_0)}{1-\theta_k(\rho, \tau)} \\ &\quad \cdot a_k(\varsigma\omega_0, (1-\varsigma)\omega_0)\varphi_k(\varsigma\omega_0, (1-\varsigma)\omega_0)\end{aligned}$$

where $\zeta = \tau(\lambda_0)/(\tau(\lambda_0) + \rho(\lambda_0)) = \tau(\lambda_0)/\omega(\lambda_0)$. The spectral variation of the coefficients ζ corresponding to two different experimental sites is shown in Fig. 5. Thus, if the kth summand of the expansion (14) at a reference leaf albedo $\omega_0 = \omega(\lambda_0)$ for different values of parameter ζ is known, the summand for any

other $\omega(\lambda)$ can be easily found. The maximum positive eigenvalue θ_0 corresponding to the positive eigenvector, can be estimated as [21]

$$\theta_0(\rho, \tau) = p\omega_\lambda = [\rho(\lambda) + \tau(\lambda)]p. \tag{17}$$

Here, $p = 1 - \exp(-K)$ where K is a wavelength independent constant.

Substituting (14) into (10) and accounting for (16) and (17), one obtains an expansion for the canopy transmittance, namely

$$t(\rho, \tau) = \left\langle \frac{1 - p\omega_0}{1 - p\omega} T_0(r_H; \varsigma, \omega_0) + \sum_{k=1}^{\infty} \frac{1 - \theta_k(\varsigma\omega_0, (1-\varsigma)\omega_0)}{1 - \theta_k(\rho, \tau)} T_k(r_H; \varsigma, \omega_0) \right\rangle_H . \tag{18}$$

Here

$$T_k(r_H; \varsigma, \omega_0) = a_k(\varsigma\omega_0, (1-\varsigma)\omega_0) \int_{\mu<0} \varphi_k(r_H, \Omega) \cdot |\mu| \, d\Omega \qquad k = 0, 1, 2, \cdots$$

Values of T_k depend on the reference hemispherical leaf albedo ω_0, the value of ζ at the reference leaf albedo, the direction of direct solar radiance Ω_0, and the points r_H. Let us consider the first term of the series (18) as a function of $\rho(\lambda)$ and $\tau(\lambda)$. That is, $T_0(\rho, \tau) = T_0(\zeta\omega_0, (1-\zeta)\omega_0)(1-p\omega_0)/(1-p\omega)$. Resolving this equation with respect to p results in (2) with $\chi = T_0$. The cumulative distribution function of p is the Heaviside function. Thus, if $\mathbf{t}(\rho, \tau) = \langle T_0(\rho, \tau)\rangle_H$, then the variable (2) is distributed in accordance with the Heaviside function. If the influence of remaining summands in (18) is sufficiently small, i.e., $\mathbf{t}(\rho, \tau) \approx \langle T_0(\rho, \tau)\rangle_H$, then the cumulative distribution function of p is close to the Heaviside function. Analysis presented in Section III indicates that $\mathbf{t}(\rho, \tau) \approx \langle T_0(\rho, \tau)\rangle_H$. It means that averaging the canopy transmittance over the angular variable, and the ground surface results in the term subscripted by 0 to be dominant in the expansion (14). However, variations in the summands caused by variation in the direction of incident solar radiation make the coefficient p sensitive to the conditions of canopy illuminations and ζ. Model calculations presented in [9] support these arguments. Thus, if the canopy transmittance at a reference leaf albedo $\omega_0 = \omega(\lambda_0)$ for different values of parameter $\zeta = \tau(\lambda_0)/\omega(\lambda_0)$ is known, the transmittance for any other $\omega(\lambda)$ can be found [Fig. 6].

It was demonstrated in Section III-B that such an interpretation is not valid for the canopy reflectance. A possible explanation is that the downward radiances result from the sum of two radiation fields. The first is the incident radiation (direct and/or diffuse) that has not interacted in the canopy and the second is the intensity of photons scattered one or more times in the canopy (the scattered component). The upward radiation field is represented by the scattered component only. Therefore, the linear operators describing canopy reflectance and transmittance are different. Clearly, these arguments are not precise and merit further consideration.

Multiplying (14) by σ and integrating over spatial and angular variables, one obtains a formula for canopy interception. It was shown [9] that the integration procedure results in only the positive term containing $a_0\varphi_0$. Moreover, the dependence of a_0 on the coefficient ζ disappears in this case. Thus, the canopy interception $\mathbf{i}(\lambda)$ and absorption $\mathbf{a}(\lambda)$ depend on the maximum eigenvalue $\theta_0 = p_i\omega(\lambda_0)$ and can be expressed by (3) and (4), respectively. Canopy absorptance, therefore, is a function of the wavelength independent coefficient p and the hemispherical leaf albedo. Resolving (4) with respect to p_i, one obtains the cumulative distribution function of ξ_i, which is the Heaviside function. Equation (4), describing the spectral variation of canopy absorptance can be derived as in Section III-B.

The following interpretation of the coefficient $p_i = 1 - \exp(-K)$ can be given. Taking $\omega(\lambda_0) = 0$ and $\omega(\lambda) = 1$ in (3), one obtains the following relationship between canopy interception and the coefficient p_i:

$$1 - p_{\mathbf{i}} = \frac{\mathbf{i}(\omega(\lambda_0) = 0)}{\mathbf{i}(\omega(\lambda) = 1)} = \frac{\int_V \int_{4\pi} \sigma(r, \Omega) I_{\omega=0}(r_0, \Omega) \, d\Omega \, dr}{\int_V \int_{4\pi} \sigma(r, \Omega) I_{\omega=1}(r_0, \Omega) \, d\Omega \, dr}.$$

The right side can be evaluated, e.g., using Monte Carlo technique [29] as the ratio N_1/N_2, where N_1 and N_2 are counts of photon interactions with absorbing ($\omega = 0$) and scattering ($\omega = \rho + \tau = 1$) leaves, respectively. For example, if the canopy is idealized as a "big horizontal leaf" then $N_1 = N_2 = 1$, i.e., $p = 0$. The ratio $\mathbf{a}(\lambda)/\mathbf{a}(\lambda_0)$ coincides with the ratio $[1-\omega(\lambda_0)]/[1-\omega(\lambda)]$ of leaf absorptances at two wavelengths. A deviation of canopy structure from the "big leaf" model involves the dependence of $\mathbf{a}(\lambda)/\mathbf{a}(\lambda_0)$ on p. Therefore, models based on the "big leaf" concept must be corrected for the effect of canopy structure.

The point p_i, at which the cumulative distribution function for the canopy interception shows a sharp increases, characterizes the two states of the vegetation canopy, that is, canopy with absorbing and scattering leaves, respectively. All intermediate states can be quantified by the wavelength-dependent maximum eigenvalue $p_{\mathbf{i}}\omega_\lambda$. Thus, an actual state of a given vegetation canopy is determined by the hemispherical leaf albedo and canopies of the same structure with absorbing and scattering leaves. The interpretation of the coefficient $p_{\mathbf{t}}$ for canopy transmittance is similar.

V. Conclusions

This paper presents empirical and theoretical analyses of spectral hemispherical reflectances and transmittances of individual leaves and vegetation canopies in the case of a dark canopy ground. The results show that spectral variations of canopy absorptance and transmittance are mainly influenced by optical properties (spectral leaf transmittance and reflectance) of individual leaves and two wavelength independent structural variables. In the case of canopy absorptance, the structural variable is determined by the capacity of the canopy of given architecture to intercept incoming solar radiation under two extreme situations, namely leaves, which 1) totally absorb and 2) totally reflect and/or transmit the incident radiation. The canopy interception capacity is quantified by the ratio N_1/N_2, where N_1 and N_2 are counts of photon interactions with absorbing and scattering leaves, respectively. In the case of canopy transmittance, this structural variable is determined by

the ratio between radiation transmitted under the same extreme conditions of completely absorbing and scattering leaves. Canopy absorptance and transmittance at red and near-IR spectral bands approximate these extreme situations well. Both structural variables are measurable parameters, i.e., they can be estimated from field measurements. An actual capacity of the canopy to transmit and absorb the incoming radiation at a given wavelength is uniquely determined by the product of the mean hemispherical leaf albedo at this wavelength and the corresponding structural variable. Simple functions that relate optical properties of individual leaves and structural variables to canopy absorptance and transmittance have been derived both from an empirical and theoretical point of view.

The 3-D radiation field in a scattering and absorbing medium bounded at the bottom by a reflecting surface can be expressed in terms of surface reflectance properties (independent of medium) and solutions of two surface independent subproblems: the radiation field in the medium calculated for a black surface and the radiation field in the same medium (bounded by the black surface) generated by anisotropic sources located at the bottom [9], [30], [31]. This representation of the radiation field does not violate the law of energy conservation within the medium [9], [30], [31]. Therefore, to quantitatively describe photon interactions between the vegetation canopy and its floor (soil and/or understory), it is important to specify those variables that determine the radiation transport through vegetation canopies when the reflection from the ground back into the canopy is zero. Such variables include information on intrinsic canopy properties. The canopy radiation regime is a function of the optical properties of individual leaves and canopy ground and two canopy structural variables. Therefore, the energy conservation of solar radiation at a given wavelength is governed by leaf and canopy ground optical properties at this wavelength and two canopy structure-dependent and wavelength-independent variables. This feature of the shortwave energy conservation in vegetation canopies provides powerful means for accurately specifying changes in canopy structure both from ground-based measurements and remotely sensed data [32].

ACKNOWLEDGMENT

The authors wish to thank Prof. F. Hallé and his team "Radeau des Cimes" for organizing the field campaign, technical help, and support. The authors also acknowledge the encouragement of Prof. Dr. W. Barthlott, University of Bonn, Bonn, Germany, and Priv. Doz. Dr. D. Anhuf, University of Mannheim, Mannheim, Germany. They would also like to give special thanks to Prof. D. Lee, Florida State University, Tallahassee, for technical and scientific help.

REFERENCES

[1] J. T. Houghton, L. G. Meira Filho, B. A. Callander, N. Harris, A. Kattenberg, and K. Maskell, Eds., *Climate Change: Report of the Intergovernmental Panel on Climate Change (IPCC)*. Cambridge, U.K.: Cambridge Univ., 1995.

[2] W. Steffen, I. Noble, J. Canadell, M. Apps, E. D. Schulze, P. G. Jarvis, D. Baldocchi, P. Ciais, W. Cramer, J. Ehleringer, G. Farquhar, C. B. Field, A. Ghazi, R. Gifford, M. Heimann, R. Houghton, P. Kabat, C. Korner, E. Lambin, S. Linder, H. A. Mooney, D. Murdiyarso, W. M. Post, I. C. Prentice, M. R. Raupach, D. S. Schimel, A. Shvidenko, and R. Valentini, "The terrestrial carbon cycle: Implications for the Kyoto Protocol," *Science*, vol. 280, pp. 1393–1397, 1998.

[3] R. B. Myneni, J. Ross, and G. Asrar, "A review on the theory of photon transport in leaf canopies in slab geometry," *Agric. For. Meteorol.*, vol. 45, pp. 1–165, 1989.

[4] J. Ross, Y. Knyazikhin, A. Kuusk, A. Marshak, and T. Nilson, *Mathematical Modeling of the Solar Radiation Transfer in Plant Canopies*. St. Peterburg, Russia: Gidrometeoizdat, 1992.

[5] D. S. Kimes, P. J. Sellers, and D. J. Dinner, "Extraction of spectral hemispherical reflectance (albedo) of surfaces from nadir and directional reflectance data," *Int. J. Remote Sensing*, vol. 8, pp. 1727–1746, 1987.

[6] P. J. Sellers, R. E. Dickinson, D. A. Randall, A. K. Betts, F. G. Hall, J. A. Berry, G. J. Collatz, A. S. Denning, H. A. Mooney, C. A. Nobre, N. Sato, C. B. Field, and A. Henderson-Sellers, "Modeling the exchanges of energy, water, and carbon between continents and the atmosphere," *Science*, vol. 275, pp. 502–509, 1997.

[7] C. O. Justice, E. Vermote, J. R. G. Townshed, R. Defries, D. P. Roy, D. K. Hall, V. V. Salomonson, J. L. Privette, G. Riggs, A. Strahler, W. Lucht, R. B. Myneni, Y. Knyazikhin, S. W. Running, R. R. Nemani, Z. Wan, A. R. Heute, W. van Leeuwen, R. E. Wolfe, L. Giglio, J.-P. Muller, P. Lewis, and M. J. Barnsley, "The moderate resolution imaging spectroradiometer (MODIS): Land remote sensing for global research," *IEEE Trans. Geosci. Remote Sensing*, vol. 36, pp. 1228–1249, July 1998.

[8] D. J. Diner, G. P. Asner, R. Davies, Y. Knyazikhin, J. P. Muller, A. W. Nolin, B. Pinty, C. B. Schaaf, and J. Stroeve, "New directions in Earth observing: Scientific application of multi-angle remote sensing," *Bull. Amer. Meteorol. Soc.*, vol. 80, pp. 2209–2228, Nov. 1999.

[9] Y. Knyazikhin, J. V. Martonchik, R. B. Myneni, D. J. Diner, and S. W. Running, "Synergistic algorithm for estimating vegetation canopy leaf area index and fraction of absorbed photosynthetically active radiation from MODIS and MISR data," *J. Geophys. Res.*, vol. 103, pp. 32 257–32 275, 1998.

[10] Y. Knyazikhin, J. V. Martonchik, D. J. Diner, R. B. Myneni, M. M. Verstraete, B. Pinty, and N. Gobron, "Estimation of vegetation canopy leaf area index and fraction of absorbed photosynthetically active radiation from atmosphere-corrected MISR data," *J. Geophys. Res.*, vol. 103, pp. 32 239–32 256, 1998.

[11] Y. Zhang, Y. Tian, Y. Knyazikhin, J. V. Martonchick, D. J. Diner, M. Leroy, and R. B. Myneni, "Prototyping of MISR LAI and FPAR algorithm with POLDER data over Africa," *IEEE Trans. Geosci. Remote Sensing*, vol. 38, pp. 2402–2418, Sept. 2000.

[12] Y. Tian, Y. Zhang, Y. Knyazikhin, R. B. Myneni, J. M. Glassy, D. Dedieu, and S. W. Running, "Prototyping of MODIS LAI and FPAR algorithm with LASUR and LANDSAT data," *IEEE Trans. Geosci. Remote Sensing*, vol. 38, pp. 2387–2401, Sept. 2000.

[13] White and K. Abernethy, *Guide to the Vegetation of the Lope Reseve Gabon*, New York: Wildlife Conservation Society, 1987.

[14] S. Engwald, J. Szarzynski, and O. Panenferov, "Biodiversity of epiphytes, forest structure and light regime of an equatorial rainforest in Gabon, Central Africa," in Biologie d'une Canopée de Forêt Tropicale Équatoriale—IV: Rapport de la Mission: Radeau des Cimes Janvier/mars, Forêt des Abeilles, Gabon, F. Hallé, Ed., 1999.

[15] H. Ellenberg, R. Mayer, and J. Schauermann, Eds., *Ökosystemforschung. Ergebnisse des Sollingprojektes 1966–1986*. Stuttgart, Germany: Verlag Eugen Ulmer, 1986.

[16] F. Hallé and O. Pascal, Eds., *Biologie Dúne Canopée de Foret Tropicale Équatoriale—II: Rapport de la Mission: Radeau des Cimes Octobre/Novembre 1991*: Réserve de Campo, Cameroun, Opération Canopée and Fondation Elf, Lyon, 1992.

[17] G. Gravenhorst, Y. Knyazikhin, J. Kranigk, G. Mießen, O. Panferov, and K.-G. Schnitzler, "Is forest albedo measured correctly," *Meteorol. Zeitschrift*, no. 8, pp. 107–114, 1999.

[18] C. S. T. Daughtry, L. L. Biehl, and K. J. Ranson, "A new technique to measure the spectral properties of conifer needles," *Remote Sens. Environ.*, vol. 27, pp. 81–91, 1989.

[19] E. M. Middleton, S. S. Chan, R. J. Rusin, and S. K. Mitchell, "Optical properties of black spruce and jack pine needles at BOREAS sites in Saskatchewan," *Can. J. Remote Sensing*, vol. 23, no. 2, pp. 108–119, 1997.

[20] P. R. Wallace, *Mathematical Analysis of Physical Problems*. New York: Dover, 1984.

[21] Y. Knyazikhin and A. Marshak, "Fundamental equations of radiative transfer in leaf canopies and iterative methods for their solution," in *Photon-Vegetation Interactions: Applications in Plant Physiology and Optical Remote Sensing*, R. B. Myneni and J. Ross, Eds. New York: Springer-Verlag, 1991, pp. 9–43.
[22] J. Ross, *The Radiation Regime and Architecture of Plant Stands*. Norwell, MA: W. Junk, 1981.
[23] R. B. Myneni, "Modeling radiative transfer and photosynthesis in three-dimensional vegetation canopies," *Agric. For. Meteorol.*, vol. 55, pp. 323–344, 1991.
[24] Y. Knyazikhin, G. Miessen, O. Panfyorov, and G. Gravenhorst, "Small-scale study of three-dimensional distribution of photosynthetically active radiation in a forest," *Agric. For. Meteorol.*, vol. 88, pp. 215–239, 1997.
[25] J. K. Shultis and R. B. Myneni, "Radiative transfer in vegetation canopies with anisotropic scattering," *J. Quant. Spectrosc. Radiat. Transf.*, vol. 39, no. 2, pp. 115–129, 1988.
[26] J. Kranigk, *Ein Model für den Strahlungstransport in Fichtenbeständen*. Göttingen, Germany: Cuvillier, 1996.
[27] V. S. Vladimirov, "Mathematical problems in the one-velocity theory of particle transport," Atomic Energy of Canada Ltd., Chalk River, ON, Canada, Tech. Rep. AECL-1661, 1963.
[28] P. I. Richards, *Manual of Mathematical Physics*. New York: Pergamon, 1959.
[29] J. Ross and A. Marshak, "Calculation of canopy bidirectional reflectance using the Monte Carlo method," *Remote Sens. Environ.*, vol. 24, pp. 213–225, 1998.
[30] Y. Knyazikhin and A. Marshak, "Mathematical aspects of BRDF modeling: Adjoint problem and Green's function," *Remote Sens. Rev.*, vol. 18, pp. 263–280, 2000.
[31] A. Marshak, Y. Knyazikhin, A. Davis, W. Wiscombe, and P. Pilewskie, "Cloud-vegetation interaction: Use of normalized difference cloud index for estimation of cloud optical thickness," *Geophys. Res. Lett.*, vol. 27, pp. 1695–1698, 2000.
[32] R. B. Myneni, C. D. Keeling, C. J. Tucker, G. Asrar, and R. R. Nemani, "Increased plant growth in the northern high latitudes from 1981 to 1991," *Nature*, vol. 386, pp. 698–702, 1997.

Oleg Panferov received the M.S. degree in meteorology/climatology from Moscow State University, Moscow, Russia, in 1991, and the Ph.D. degree in ecology and biology from the A.N. Severtsov Institute of Problems of Ecology and Evolution, the Russian Academy of Sciences, Moscow, Russia, in 2000.

From 1991 to 1992, he was a Research Scientist with the Institute of Evolutionary Morphology and Ecology of Animals, the Russian Academy of Science, Moscow, Russia. He was a Gottlieb Daimler and Karl Benz Fellow from 1993 to 1994. Since, he has been working as a Research Scientist at the University of Göttingen, Göttingen, Germany. His research interests are modeling and measuring radiative regime and photosynthesis in plant canopies, optical properties of vegetation, and remote sensing of vegetation.

Yuri Knyazikhin received the M.S. degree in applied mathematics from Tartu University, Tartu, Estonia, and the Ph.D. degree in numerical analysis from the N.I. Muskhelishvilli Institute of Computing Mathematics, the Georgian Academy of Sciences, Tbilisi, Georgia, in 1978 and 1985, respectively.

He was a Research Scientist with the Institute of Astrophysics and Atmospheric Physics and Tartu University, Computer Center of the Siberian Branch of the Russian Academy of Sciences, Novosibirsk, Russia, from 1978 to 1990. He was an Alexander von Humboldt Fellow from 1992 to 1993, and worked at the University of Göttingen, Göttingen, Germany, from 1990 to 1996. He is currently a Research Associate Professor in the Department of Geography, Boston University, Boston, MA. He has worked and published in areas of numerical integral and differential equations, theory of radiation transfer in atmospheres and plant canopies, remote sensing of the atmosphere and plant canopies, ground-based radiation measurements, forest ecosystem dynamics and modeling sustainable multifunctional forest management.

Ranga B. Myneni received the Ph.D. degree in biology from the University of Antwerp, Antwerp, Belgium, in 1985.

Since then, he has worked at Kansas State University, Manhattan, the University of Göttingen, Göttingen, Germany, and NASA Goddard Space Flight Center, Greenbelt, MD. He is now on the Faculty of the Department of Geography, Boston University, Boston, MA. His research interests are radiative transfer, remote sensing of vegetation, and climate-vegetation dynamics. He is a MODIS and MISR Science Team Member.

Jörg Szarzynski received the M.S. degree in geography and biology from the Rheinische Friedrich-Wilhelms-University of Bonn (RFA), Bonn, Germany, in 1994, writing his thesis on microclimatological investigations on inselbergs in Taï-Nationalpark, Côte d'Ivoire, West Africa. His Ph.D. dissertation and further scientific interests are focused on forest microclimate and biophysical interactions between vegetation and the atmosphere.

From 1994 to 1995, he was a Research Scientist with the Department of Climatology and Remote Sensing, led by Prof. Dr. M. Winiger, Bonn (RFA). In 1995, he joined the scientific team of Priv. Doz. Dr. D. Anhuf, Geographical Institute of the University of Mannheim, Mannheim, Germany, who among others is responsible for the meteorological and hydrological monitoring in frame of the Surumoni crane project, an interdisciplinary research facility in the Amazonian part of Southern Venezuela.

Stefan Engwald received the Diploma degree in biology and horticulture from the Technical University of Berlin (RFA), Berlin, Germany, in 1994, writing his Diploma thesis about cultivation and selected ecological investigations on "cape gooseberry" (*Physalis peruviana* L. Solanaceae), a tropical fruit of the Andes.

In the same year, he joined the working group of Prof. Dr. W. Barthlott, Botanical Institute of the University of Bonn (RFA), Bonn, Germany, as a Member of the Scientific Staff. Here, he started working on his Ph.D. dissertation toward biodiversity and ecology of vascular epiphytes in a montane and a lowland rainforest in Venezuela (Surumoni crane project). After gaining experiences within the framework of a forest decline research program with scots pine forests near Berlin, he conducted various field studies in Sweden, Costa Rica, Venezuela, and Gabon. He is scientifically interested in aspects concerning (tropical) forest structure and ecology, spatial distribution, and bioindicative potential of plants.

Karl G. Schnitzler received the Diploma and Ph.D. in physics from the Georg-August-University Göttingen, Germany, in 1994 and 1999, respectively.

He had been actively involved in studies of the vertical exchange of reactive trace gases between the troposphere and the terrestrial biosphere as well as studies of the behavior of nitrogen and sulphur compounds over the Atlantic ocean. He is currently a Postdoctoral Researcher with the Max-Planck-Institute for Meteorology, Hamburg, Germany, where he studies biosphere-atmosphere interactions and their role in the global carbon cycle.

Gode Gravenhorst received the M.S. and Ph.D. degrees in meteorology from the J.W. Goethe University, Frankfurt, Germany.

He has worked at research institutes in the United States, France, and Germany on trace substances in the atmosphere and their interactions with the biosphere. Currently, he is the Head of Institute of Bioclimatology, Faculty for Forestry and Ecosystem Research, University of Göttingen, Göttingen, Germany, and the Head of the Center for Tropical and Subtropical Agriculture and Forestry. He was Acting Lead of the Research Center for Forest Ecosystems. His research interests are now energy and mass exchange between forests and atmosphere and its influence on functioning of forest ecosystems and atmospheric boundary layer.